Measurements of Underground and Underwater Temperatures by Quartz Thermometers at Syowa Station, East Antarctica

Kazuo SHIBUYA*, Toshiyasu NAGAO**
and Katsutada KAMINUMA*

水晶温度計を用いた昭和基地での地中および海水温度の精密連続測定

渋谷和雄*・長尾年恭**・神沼克伊*

要旨: 8カ月間の地中温度連続観測が，昭和基地の20 m岩盤ボーリング孔を用いて行われた．特別に設計された水晶温度計による観測の結果，深さ5 mでは−4.89°Cから−10.36°C (変動幅5.47°C) の間で正弦関数的な変動を示すことがわかった．上記の変動幅は10 mの深さでは1.58°C (−7.73°C～−9.31°C) となり，20 mの深さでは0.20°C (−8.17°C～−8.37°C) となる．気温の季節変動にくらべ地中温度の極大，極小の表れる時期には位相の遅れが生じるが，その値は深さ5 mで約90日，深さ20 mでは約290日に達することがわかった．また，気象変動が地中温度に及ぼす影響に，指数関数的な減衰をあてはめると33.8 mの深さで0.01°Cの変動幅におさまるはずである．海水温の連続測定も6カ月間にわたり，オングル島西の浦の海氷下7 mの海水中で行われた．それによると6月上旬の−1.63°Cから11月下旬の−1.48°Cまで大体0.9×10^{-3} °C/日の割合で海水温は上昇した．さらに上記の傾向にかぶさるように10–30日の短かい周期を持つ0.05–0.10°Cの変動が認められ，それは突然温度が上昇し，その後ゆるやかに下降していくパターンの繰り返しで特徴づけられる．

Abstract: Eight-months' observation of underground temperature was made by specially designed quartz thermometers in a 20 m borehole at Syowa Station, East Antarctica. The underground temperature at 5 m depth showed a quasi-sinusoidal change of 5.47°C from −4.89°C to −10.36°C. The above change became smaller to 1.58°C in the range of −7.73°C～−9.31°C at 10 m depth, and became further smaller to 0.20°C in the range of −8.17°C～−8.37°C at 20 m depth. In comparison with the seasonal variation of air temperature, there was a phase delay of about 90 days at 5 m depth and about 290 days at 20 m depth. The effect of the seasonal variation of air temperature on that of underground temperature can be estimated as less than 0.01°C at the depth of 33.8 m when exponential decay against depth is assumed to have resulted from such effect. Six-months' observation of sea-water temperature was also made at 7 m depth under the ice-cover of the coast of Nisi-no-ura Cove. The observation revealed a gradual increase of temperature from −1.63°C in June to −1.48°C in November at an approximate rate of 0.9×10^{-3} °C/day. Superposed on the above long-term trend, there was a sequence of short-term (10–30 days) variations of 0.05–0.10°C which was characterized by the abrupt increase and the subsequent gradual decrease of temperature.

* 国立極地研究所. National Institute of Polar Research, 9-10, Kaga 1-chome, Itabashi-ku, Tokyo 173.

** 千葉大学理学部. Faculty of Science, Chiba University, 1-33, Yayoi-cho, Chiba 260.

1. Introduction

Though space and time variations of underground and underwater temperatures are important factors in the study of physical oceanography, meteorology and solid earth physics in the antarctic region, there were not many cases of yearlong observations of such. Since we have limited knowledge on the thermal processes of geophysical phenomena in the antarctic region, temperature measurements with a wide dynamic range and wide frequency response are required. The yearlong measurements with a resolution of 1×10^{-3} °C (hereafter we denote sometimes 1×10^{-3} °C as 1 m°C) and relative accuracy of 10 m°C may give us information on the hitherto overlooked phenomena. The thermometer has also to be so designed that it can be installed and maintained easily. A quartz thermometer which satisfies the above requirements has been developed by SHIMAMURA (1980) and applied by the 21st Japanese Antarctic Research Expedition (JARE-21) to the long-

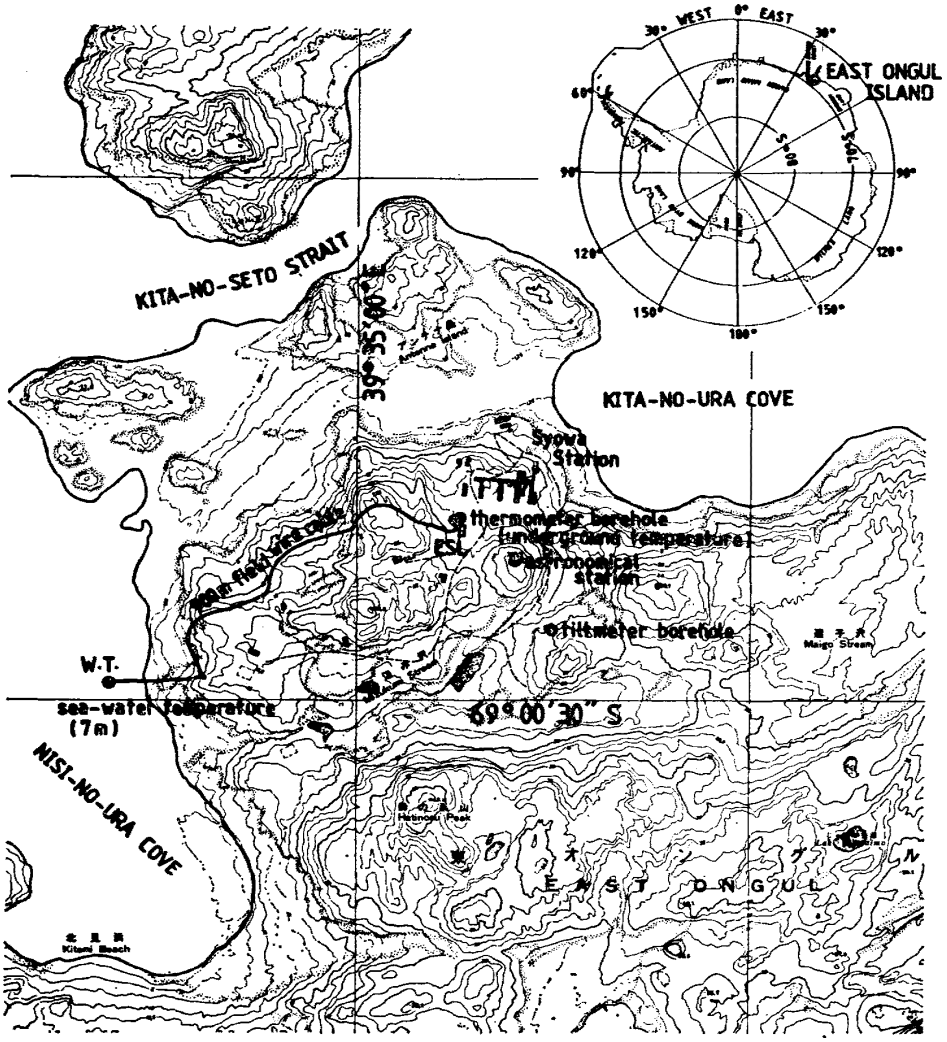

Fig. 1. The location of quartz thermometers installed by JARE-21 on East Ongul Island. The borehole site is near the Earth Science Laboratory. W. T. denotes the observation site of sea-water temperature.

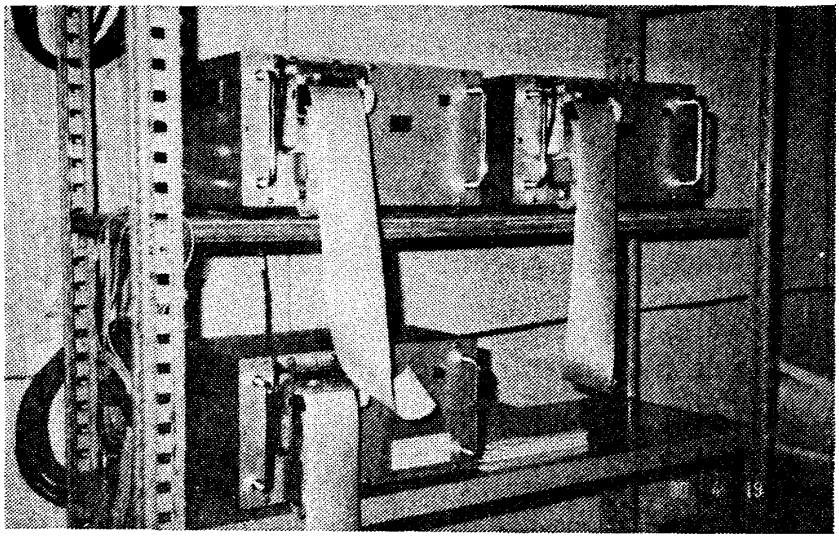

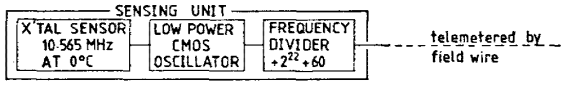

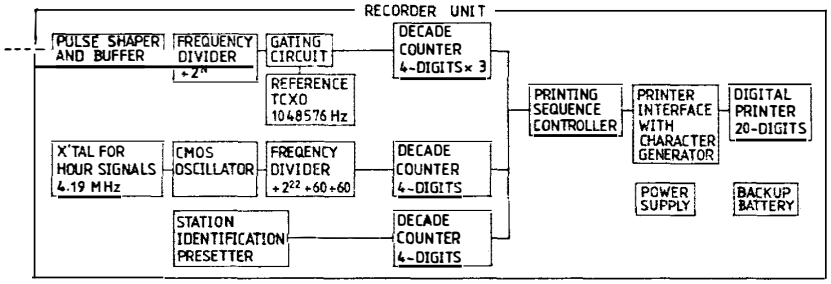

Fig. 2. Upper part shows the appearance of the recorder. Frequency counts are output on a dot printer. Lower part shows the block diagram of the system, redrawn from SHIMAMURA *(1980).*

term observations of underground and underwater temperatures at East Ongul Island, East Antarctica.

Figure 1 illustrates the location of the installed quartz thermometers on East Ongul Island. Air drilling was made by two members of JARE-21 during the austral summer on February 1–March 22, 1980 and a borehole of 20 meters deep with a diameter of 50 mm was obtained at the site near the Earth Science Laboratory (ESL). Though four quartz sensors were suspended in air in the drilled borehole at intervals of 5 meters from 5 m depth to 20 m depth, the 15 m sensor was found broken after the installation. The cable length of each sensor-recorder system was 100–150 m. A quartz sensor was also installed at the depth of 7 m under sea-ice cover on the coast of Nisi-no-ura Cove, as denoted by the mark W.T. in Fig. 1. Since the sensing unit is suspended in sea-water without being anchored to the sea bottom, there may be slight time variations of depth by the stream. The cable of about 900 m was lined between Nisi-no-ura Cove and the ESL, and the recorder could be maintained by AC power at the laboratory. Figure 2 illustrates the appearance of the recorders in the ESL and the block dia-

gram of the installed sensor-recorder systems which was redrawn from SHIMAMURA (1980). One of the most significant advantages of the system is that the signals from the sensing unit can be telemetered by the twisted field wire instead of coaxial cables of limited length (approximately 30–50 m) for commercial quartz thermometers.

2. System Calibration

The principle of the installed quartz thermometer is essentially a frequency counter. Since the detailed circuit design and the performance are described in SHIMAMURA (1980), only the outline is reviewed here. The sensing quartz crystal generates almost linear temperature-dependent frequencies in the temperature range of $-50°C \sim +100°C$ at the change rate of approximately 985 Hz/°C and about 10.56 MHz at 0°C. The generated frequencies are divided into the rectangular wave of about 50 s period at the sensing unit. The rectangular wave is telemetered by the twisted field wire to the recorder unit and the reference frequencies of TCXO (temperature compensated X'tal oscillator) in the recorder unit are counted by using the telemetered rectangular wave as the gate (see the block diagram in Fig. 2). Since the temperature-dependence of the sensing quartz is positive, the width of the gate becomes smaller as the temperature becomes higher, which results in smaller frequency counts.

The stability and the accuracy of the system depend mainly on the accuracy and

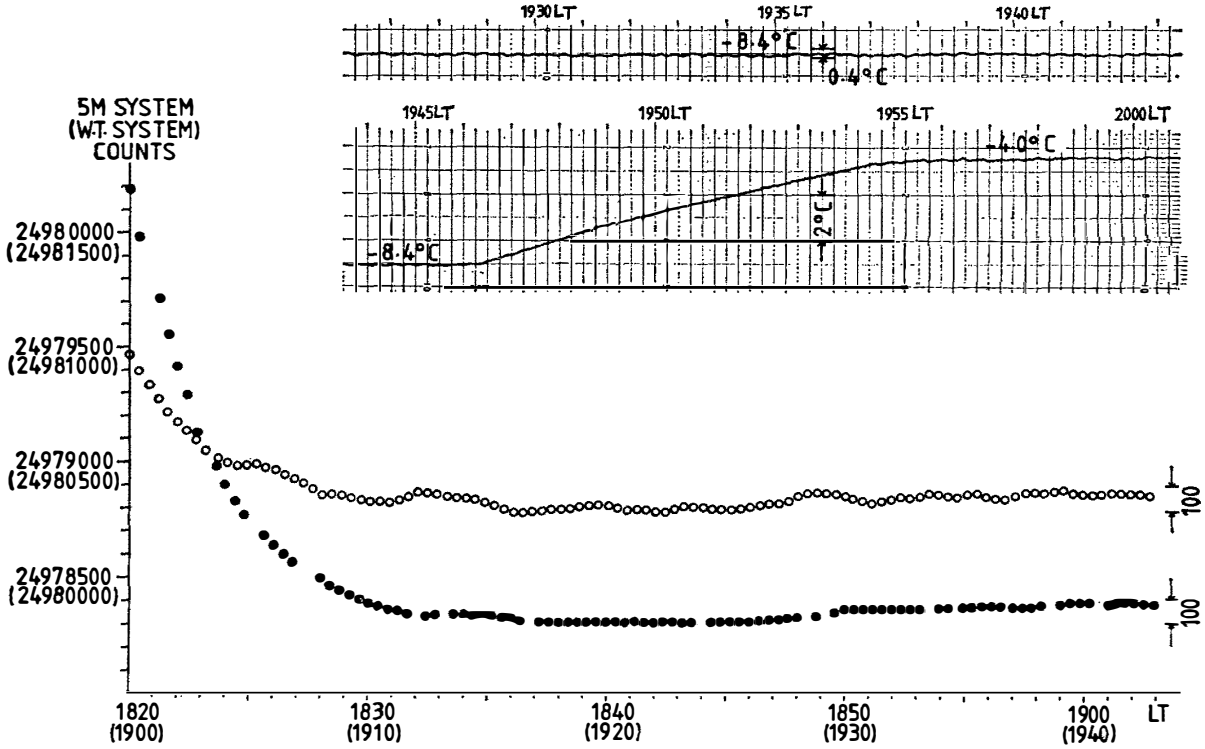

Fig. 3. Upper part illustrates the temperature control of the thermostatic bath at −8.4° C. Lower part gives the corresponding change of the frequency counts when the temperature of the thermostatic bath is raised from −12° C to −8.4° C. Solid circle . . . 5 m system. Open circle . . . W.T. system. Numerals in parentheses are the co-ordinate values for the W.T. system.

the stability of TCXO. They also depend on the accuracy and the stability of the triggered point of the telemetered rectangular wave, since the edge of the pulse is not ideally sharp. The calibration of the above quartz thermometer is to be made by the overall system including sensing unit, telemetered cable, TCXO, and the counting circuits. After 8 months' observation, we recovered the whole systems and made calibration tests by using a HAAKE cryostat. Figure 3 (upper part) gives an example of the analog monitor record of the temperature variation in the thermostatic bath when the temperature of methyl alcohol solution was raised from about $-12°C$ to $-8.4°C$ at 1816LT and was controlled at the value for 90 minutes, then was raised further from $-8.4°C$ to $-4.0°C$ at 1946LT and again was controlled at $-4.0°C$. The temperature values were read by a standard mercury thermometer, which has the absolute accuracy of $0.1°C$, to the resolution of $0.05°C$ by using a magnifying glass every 5 minutes. Solid circles in Fig. 3 (lower part) show the change of frequency counts of the system used in the measurement of underground temperature at 5 m depth (5 m system), which correspond to the temperature variation from 1830LT to 1916LT during the system calibration. Likewise, open circles in Fig. 3 (lower part) give the change of frequency counts for the system used in the temperature observation of sea-water (W.T. system) and correspond to 1900LT–1946LT. The sensing unit of the 5 m system was contained in a polyvynil container of 35 mm diameter and 55 mm length which was filled with silicon oil, while that of the W.T. system was contained in a duralumin pressure case (about 1.5 kg) of much larger volume. As the result,

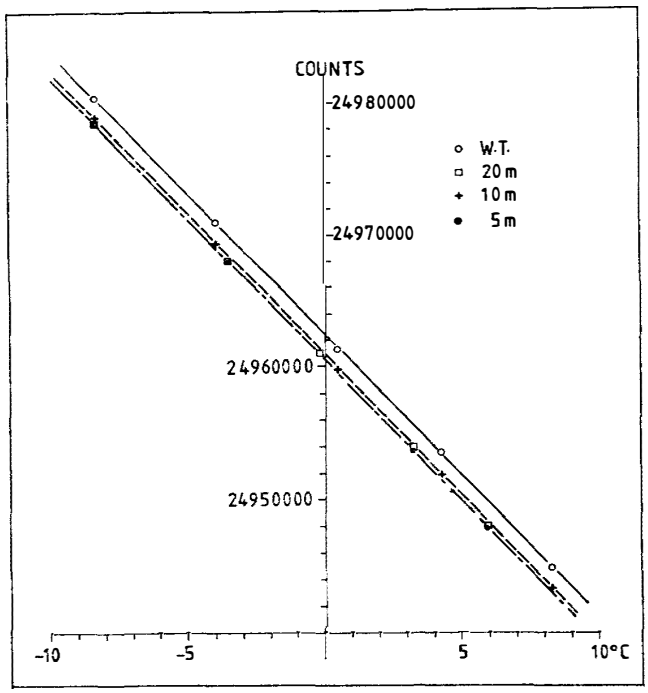

W.T. system	$F_0 = 24962400 \pm 100$
5 m system	$F_0 = 24960600 \pm 100$
10 m system	$F_0 = 24960900 \pm 100$
20 m system	$F_0 = 24960600 \pm 100$

Fig. 4. The frequency count versus temperature relation. F_0 means the frequency count at $0°C$.

the frequency counts decreased with the different time constant of 10–15 minutes for the 5 m system and 60–70 minutes for the W.T. system as the temperature of thermostatic bath approached from −12°C to −8.4°C. As shown in the upper part of Fig. 3, the thermostatic bath cannot be controlled better than the range of 0.1°C around −8.4°C, which resulted in the fluctuations of 100 frequency counts around 24978250 for the 5 m system and around 24980340 for the W.T. system as shown in the lower part of Fig. 3.

Similar calibration tests for the whole installed quartz thermometer systems were made at other four selected temperature values within the range −10°C～+10°C. Figure 4 summarizes the frequency counts *versus* temperature relation for each system, where open circle, open box, cross and solid circle denote W.T. system, 20 m system, 10 m system and 5 m system, respectively. The frequency counts are ascertained to have a rather strict linear dependence on temperature with the change rate of -2.0 ± 0.05 count/m°C for the whole installed systems. The frequency count at 0°C, F_0, has some offsets among the systems, which is considered to have resulted from the overall effects of the slight inconsistence of the frequency characteristic of the quartz crystal in the sensing unit, the reference frequency of TCXO in each recorder, the uncertainty of the temperature control of the cryostat, reading resolution of the standard mercury thermometer, etc. The value of F_0 for each system is also listed in Fig. 4. Though the uncertainty of 100 counts in F_0 results in the uncertainty of ±50 m°C in the absolute accuracy of the transformed temperature, relative accuracy within 10 m°C at each system is ascertained by both the resolution of 0.5 m°C/count and the long-term stability of the data shown in the next section.

3. Results and Discussion

The observation of underground temperatures was made from April 17, 1980 to January 2, 1981, while that of underwater temperatures was made from June 9, 1980 to January 2, 1981. Figure 5 illustrates an example of the output print of the frequency counts from the 20 m system on August 1, 1980. The output was made at intervals of about 50 minutes by summing up each of the frequency counts in the 64 rectangular gates. The frequency count frame (5th to 14th digits) in Fig. 5 can be considered as giving an average of the temperature variations in the interval of about 50 minutes as illustrated in the right-hand side of the figure. The third digit in the count frame (digit number 7) corresponds to the digit of 1 m°C in the transformed temperature. It is noted that the temperature resolution in the above time interval exceeds 0.1 m°C remarkably following the long-period and small change of temperature. Output prints in 8 months' observation were compiled in one volume of magnetic tape and the frequency counts were transformed to the temperature after the formula expressed in the appendix.

Figure 6 (upper part) plots every 32 hours' interval data in the observation of underground temperatures. Symbols X, Y and Z denote temperatures at 5 m depth, 10 m depth and 20 m depth, respectively. At 5 m depth, the underground temperature showed a quasi-sinusoidal change in the range from about −4.89°C

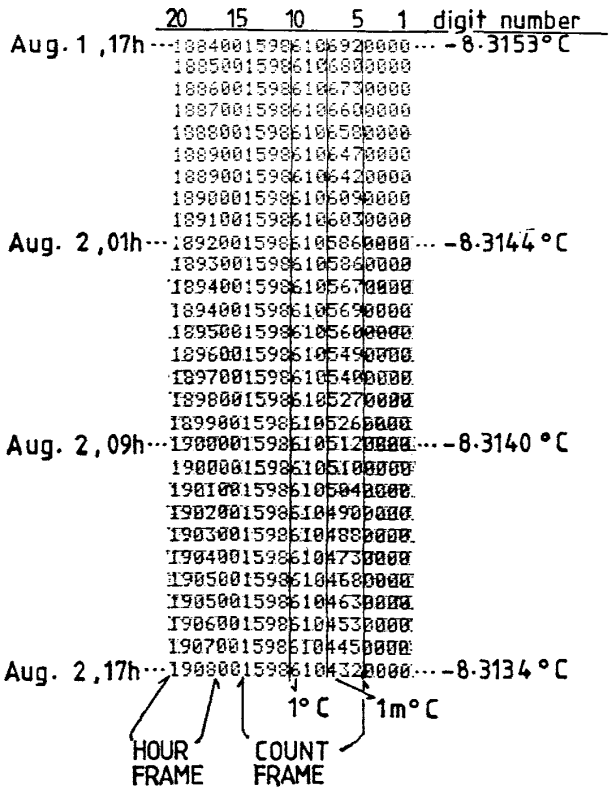

Fig. 5. An example of the output from a dot printer. See the text.

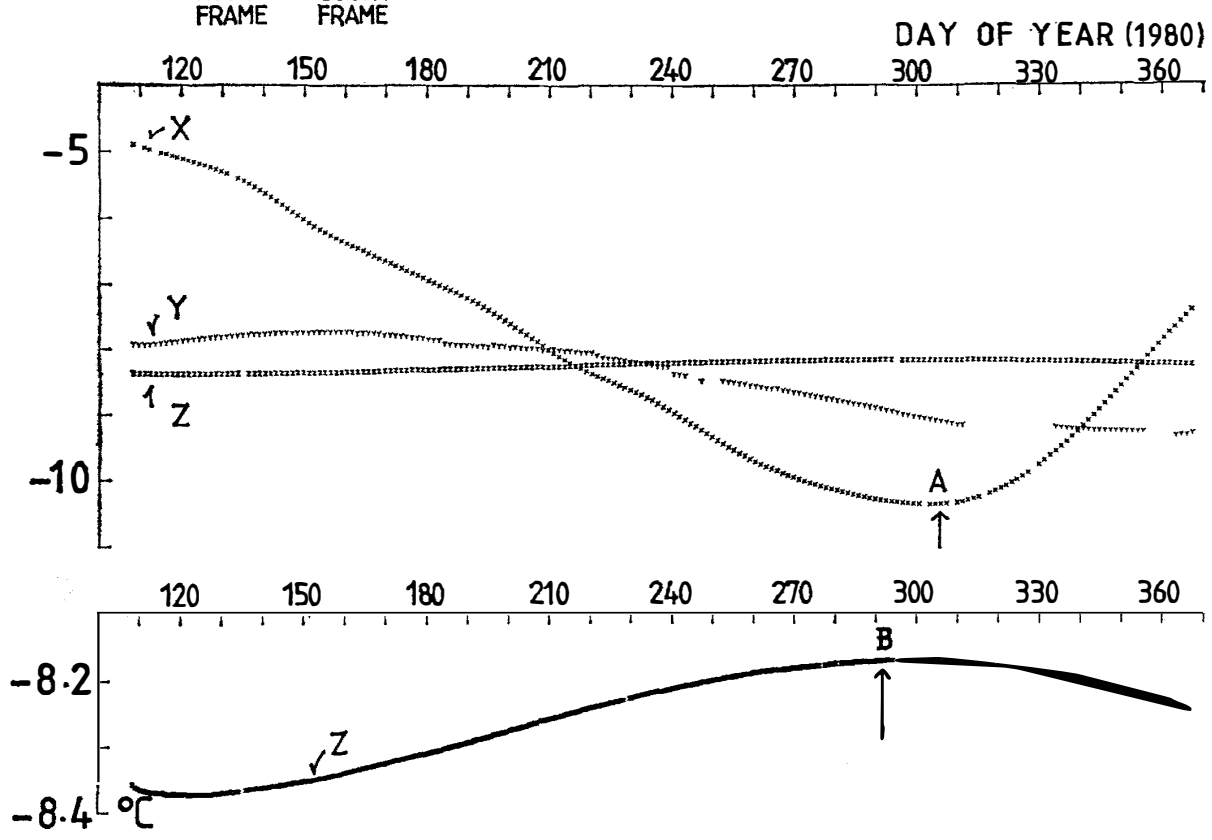

Fig. 6. The 32 hours' interval plots of underground temperature in April-December, 1980. X, Y and Z denote temperatures at 5 m depth, 10 m depth and 20 m depth, respectively. As for 20 m depth, 16 hours' interval plots in an enlarged scale of the ordinate are given in the lower part. A- and B-arrows correspond to the minimum at 5 m depth and the maximum at 20 m depth in the seasonal trends, respectively.

(the maximum is out of the observation period) to −10.36°C (the minimum is around 300 day of year), while that at 10 m depth changed from −7.73°C (the maximum around 150 day of year) to about −9.31°C (the minimum probably around 360 day of year). Though the temperature at 20 m depth looks almost constant in the upper part of Fig. 6, the enlargement of the scale of the ordinate and the plot with every 16 hours' interval (lower part of Fig. 6) clearly shows a sinusoidal change of temperature from −8.17°C (the maximum around 290 day of year) to −8.37°C (the minimum around 110 day of year). In order to see the correlation of underground temperature with the air temperature, 10 days' running means of both daily maximum and daily minimum air temperatures, which are considered to give enhanced seasonal variations of air temperatures by suppressing daily variations, in two years (January 1979–December 1980) are calculated and plotted in Fig. 7 with symbols U and L, respectively. Considering the trends connecting U or L in Fig. 7, peaks in such seasonal variation of air temperatures appear around 0–10 day of year with the range of −2°C∼+5°C, while troughs appear around 230–240 day of year with the range of −25°C∼−15°C. Comparison of Fig. 6 with Fig. 7 indicates that the phase delay of underground temperature variation at 5 m depth against the seasonal trend of air temperature variations is about 90 days as shown by the difference of the day of year marked by two A-arrows in Figs. 6 and 7. The above delay is not distinct at 10 m depth, partly because of the lack of observations before 120 day of year and 310–330 day of year in Fig. 6. The delay amounts to about 290 days for the underground temperature at 20 m depth (see also the difference of the day of year marked by B-arrows). Considering the ranges of the variation of underground temperature, about 5.47°C at 5 m depth, about 1.58°C at 10 m depth and 0.20°C at 20 m depth, and assuming exponential decay of such variations which may be the results of

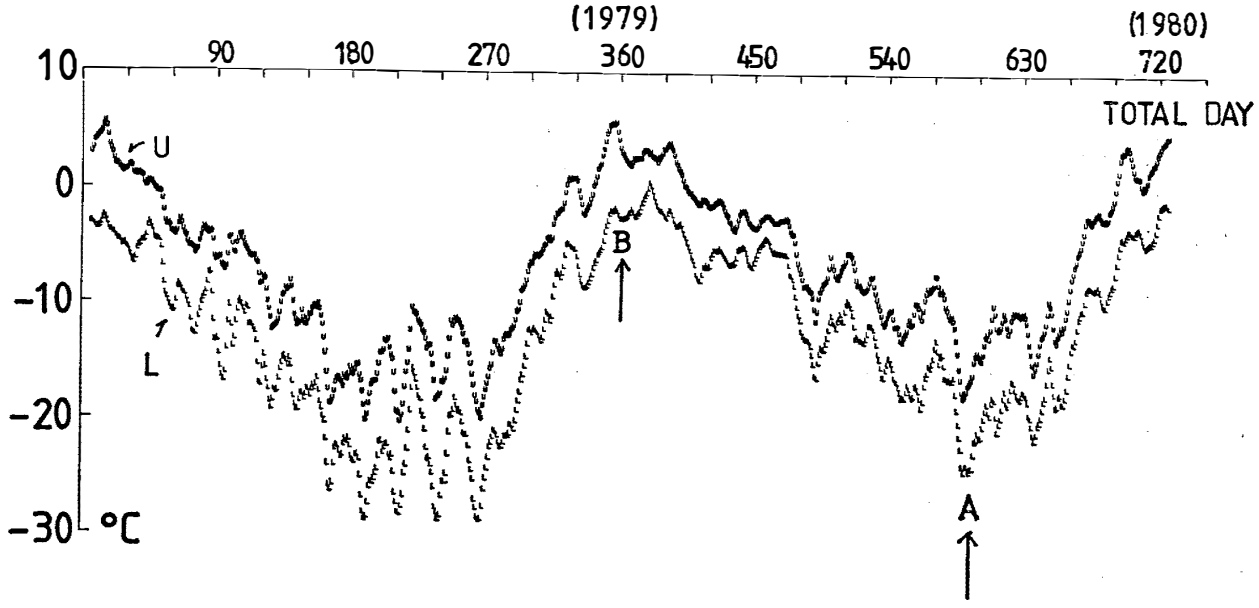

Fig. 7. The 10 days' running mean of daily maximum air temperature (symbol U) and that of daily minimum air temperature (symbol L). A- and B-arrows correspond to the minimum and the maximum in the seasonal trends of air temperature in 1980, respectively. Total day is counted from January 1, 1979 to December 31, 1980.

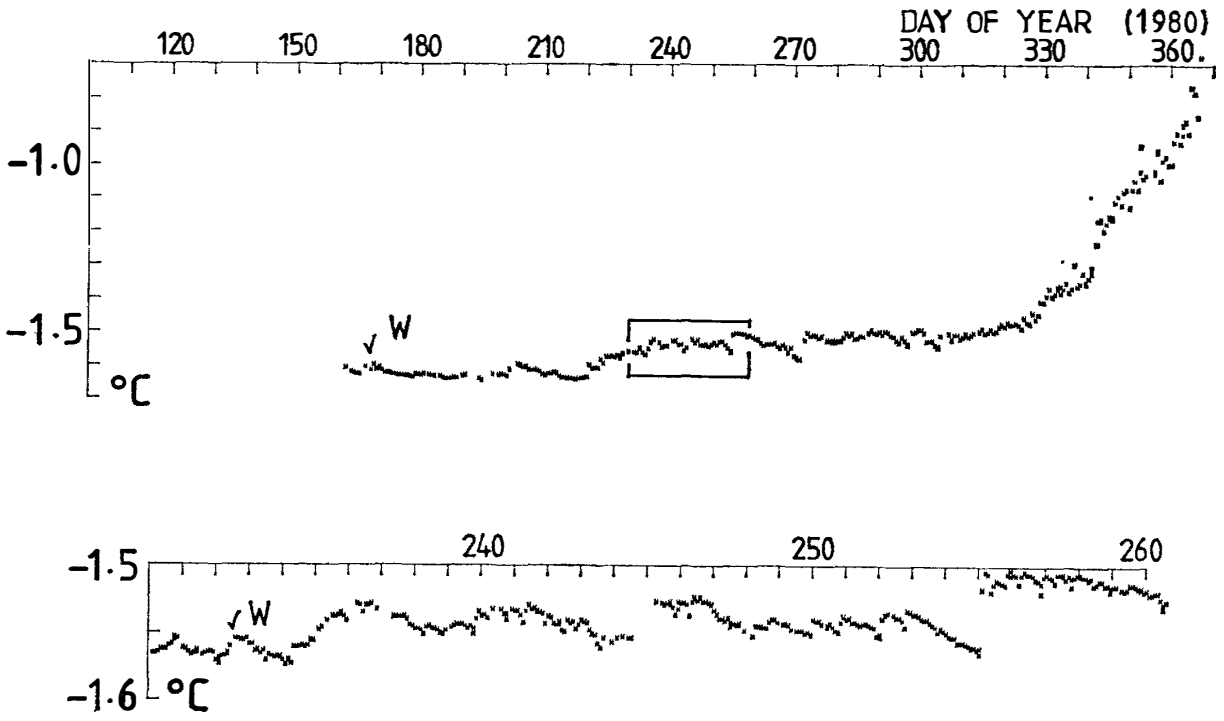

Fig. 8. Temperature variation of sea-water at 7 m depth under ice-cover on the coast of Nisi-no-ura Cove (symbol W). 2 hours' interval plots of the variation during 230–260 day of year (the box in the upper part) are given in an enlarged scale of the ordinate in the lower part of the figure.

the effect of seasonal change of air temperature, the effect will be less than 10 m°C at the depth of 33.8 m.

The upper part of Fig. 8 displays underwater temperature variation. The temperature of sea-water became gradually higher from −1.63°C (around 160 day of year) to −1.48°C (around 330 day of year) at the approximate rate of 0.9 m°C/day. There seems to be also fine structures with the change order of 50–100 m°C on the above trend, as shown by the sequence of abrupt increase and subsequent gradual decrease of temperature which is illustrated in the lower part of Fig. 8 by more detailed plots of every 2 hours' interval during 230–260 day of year. The phenomena may be related to the physical processes of sea-water sea-ice interactions or short-period seasonal variation of air temperature in Fig. 7. There was a steep increase of temperature from −1.48°C to −0.70°C during 40 days of 330–370 day of year, which may result from the inflow of fresh water from melted snow on the coast of Nisi-no-ura Cove.

4. Application of Quartz Thermometers for Future Research

Originally, the air drilling was planned to obtain a 50–100 m borehole on East Ongul Island. However, difficulties of logistics and operations in bad weather prevented us from accomplishing the object. As shown in the former section or predicted by the results of the underground temperature observations in lower latitudes, the effect of seasonal variation of air temperature on the underground temperature variation will be within the range of 10 m°C at the depth of 33.8 m.

If we take tentative value of $Q=0.5-2.0\times10^{-2}\times J$ W/m^2 for heat flow in the antarctic region and $k=2-4\times10^{-1}\times J$ W/m°C for thermal conductivity (*e.g.*, GERARD *et al.*, 1962) where J is Joule's constant, then the temperature gradient against depth $\Delta T/\Delta h$ is given by

$$\Delta T/\Delta h=\frac{Q}{k}=\frac{0.5-2.0\times10^{-2}\times J \text{ W/m}^2}{2-4\times10^{-1}\times J \text{ W/m°C}}$$
$$=0.1-1.0\times10^{-1} \text{ °C/m}$$
$$=10-100 \text{ m°C/m}.$$

Though relative accuracy of quartz thermometers can be improved by using the same TCXO for two or more sensing units, at least 200 m°C of ΔT is required for precise measurements of heat flow, which results in the necessity for the depth interval Δh of 2–20 m and consequently total depth of 50 m.

One of the most adequate and fruitful utilizations of quartz thermometers is the unmanned long-term temperature measurement of sea-water. Figure 9 illustrates an example of the temperature measurements of sea-water at various points and depths in Lützow-Holm Bay by the portable quartz thermometer of the same

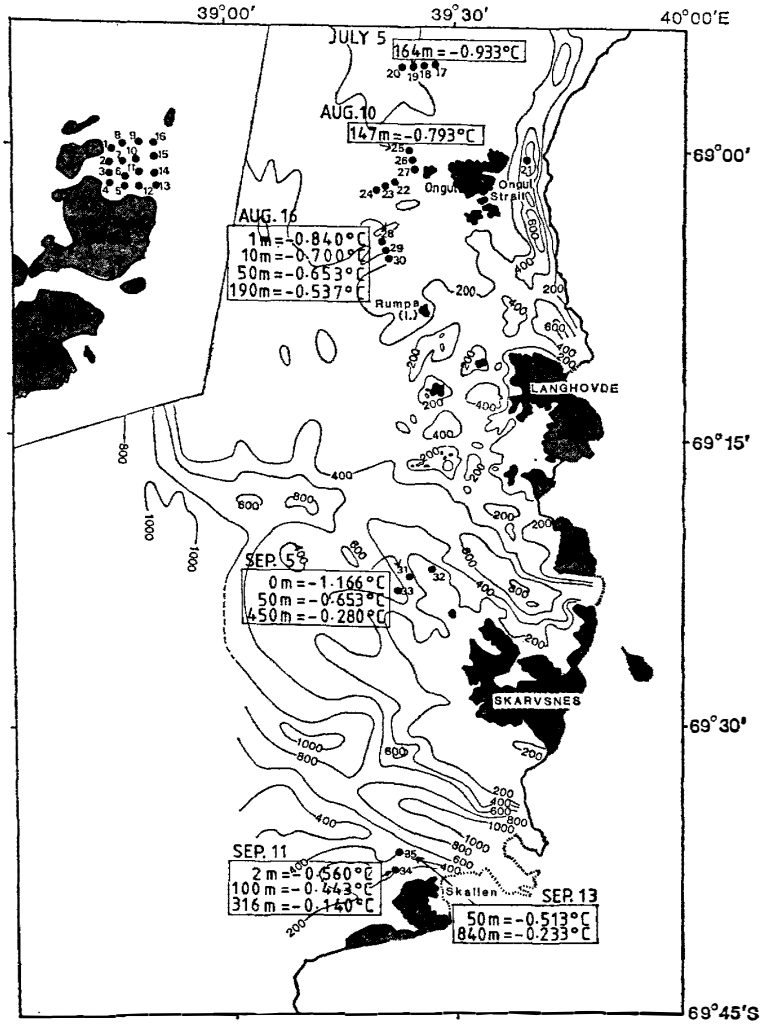

Fig. 9. Log data of underwater temperatures in Lützow-Holm Bay. The lowest (or the only one) column in each box shows the temperature at the sea bottom.

design as that of the W.T. system. As the date of measurements ranges mostly from August 10 to September 11, and as the depth of the bottom ranges from 150 m to 840 m, an accurate comparison of the obtained temperatures at different points is impossible. However, Fig. 9 suggests higher temperature fields in the southern part against the northern part under the ice-cover of Lützow-Holm Bay in August or September, and the yearlong installation of many such quartz thermometers may reveal seasonally systematic or geographically dependent temperature structures.

Acknowledgments

The authors express their sincere thanks to Messrs. R. KATO and S. KATAOKA of JARE-21, who, in spite of the logistic and operational difficulties and their non-specialty, devoted themselves to the drilling till the whole drilling bits were used up. One of the authors (K. SHIBUYA) also thanks Drs. S. KAWAGUCHI and Y. NAITO and all the members of JARE-21 for their assistance and encouragement during the wintering. Dr. H. SHIMAMURA kindly instructed us how to appropriately install and maintain the quartz thermometers. The Institute of Low Temperature Science, Hokkaido University kindly let us use a HAAKE cryostat. This research was partly financed by the budget for JARE, entitled to the "Geophysical investigation of the crust and upper-mantle structures of the Prince Olav Coast, East Antarctica (representative: T. NAGATA)".

References

GERARD, R., LANGSETH, M.G., JR. and EWING, M. (1962): Thermal gradient measurements in the water and bottom sediment of the Western Atlantic. J. Geophys. Res., **67**, 785–803.

SHIMAMURA, H. (1980): Precision quartz thermometers for borehole observations. J. Phys. Earth, **28**, 243–260.

(Received April 5, 1982; Revised manuscript received May 19, 1982)

Appendix

The frequency counts F_T of underground sensors are mostly expressed by $F_T=1598000000+F$, where F is positive integer of 6 digits. Dividing F_T by 64, the frequency count F_T' in one rectangular gate is expressed by

$$F_T'=24968750+F', \tag{1}$$

where

$$F'=F/64. \tag{2}$$

Following the relation in Fig. 4 of the text, $F_T'=F_0-\alpha T$, where α is the change rate of counts against temperature and is approximately 2.1×10^3 counts/°C. Substitution of 24960600 for F_0 of the 5 m system finally results in

$$T=0.47\times\{60600-(68750+F')\}\ \text{m°C}. \tag{3}$$

Similar expressions are obtained for 10 m and 20 m underground temperatures. As for the W.T. system, the frequency counts are expressed by $F_{T,WT}=1597000000+F$. Similar procedures finally give the underwater temperature which is expressed by

$$T=0.47\times\{62400-(53125+F')\}\,\mathrm{m°C}, \qquad (3)'$$

instead of eq. (3).

In the compiled magnetic tape, total hours from the start (ITIME), fractional frequency counts F' (IFREQ) and transformed temperature in m°C (ITEMP) are written sequentially by the specification and the data format which are illustrated in Fig. A-1.

(1) Magnetic tape with a standard label

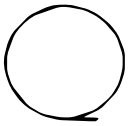

VOL=SER=HEAT21

(2) Multi-file compilation

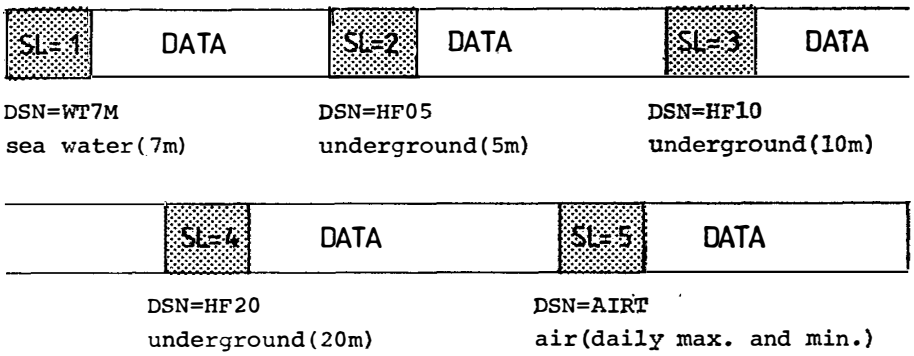

(3) Data format(SL=1-4)

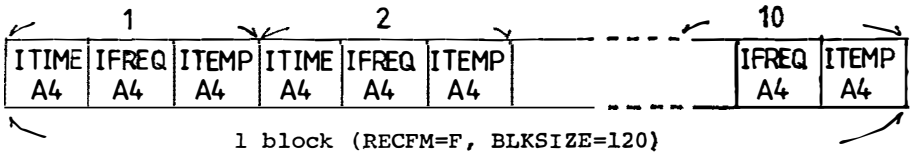

ITIME ... total hours from the start
IFREQ ... fractional frequency counts, eq. (2) in the appendix
ITEMP ... temperature in m°C

(4) Data format(SL=5)

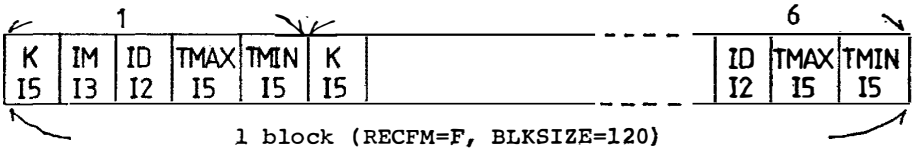

K ... day of year
IM ... month
ID ... day
TMAX ... daily maximum air temperature
TMIN ... daily minimum air temperature

by JARE-20 and -21

Fig. A-1.